**Supporting Information**

# The pH-dependent Structures of the Manganese Binding Sites in Oxalate Decarboxylase as Revealed by High-Field Electron Paramagnetic Resonance.

Leandro C. Tabares[a], Jessica Gätjens[a,b], Christelle Hureau[a], Matthew R. Burrell[d], Laura Bowater[c], Vincent L. Pecoraro[b], Stephen Bornemann[c] and Sun Un[a]*

[a]Service de Bioénergétique, Biologie Structurale et Mécanismes, Institut de Biologie et Technologies de Saclay, CNRS URA 2096, CEA Saclay, 91191 Gif-sur-Yvette, France.

[b]Department of Chemistry, University of Michigan, Ann Arbor, MI 48109-1055, USA.

[c]Biological Chemistry Department, John Innes Centre, Norwich Research Park, Colney, Norwich NR4 7UH, United Kingdom.

Email: sun.un@cea.fr

## 1. pH dependence of the activity of the C-terminal his-tagged OxdC

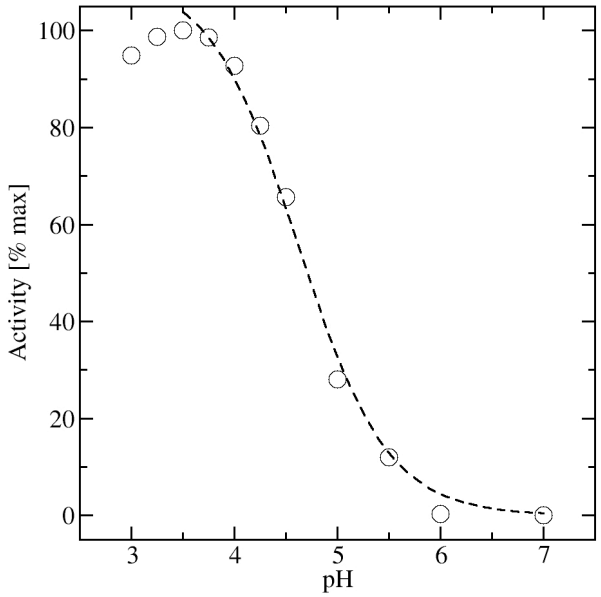


**Figure S1.** The pH dependence of the C-terminal his-tagged OxdC. Assay conditions: 100 mM citrate and 150 mM oxalate (see ref 29 for experimental details). A $pK_a$ of 4.6 was determined from a fit of the data based on the equation $A=A_0/(1+K_a/[H])$ where A is the percent activity.

## 2. Detailed description of the HFEPR of Mn(II) centers

At the heart of our study was the measurement of the Mn(II) zero-field interaction of the two OxdC Mn(II) sites. The zero-field interaction is traditionally characterized by two parameters *D* and *E* and is one of three magnetic interactions that a Mn(II) ion experiences. The effects of the three interactions are given by:

$$H = g\beta BS_z + AI_zS_z + \frac{D}{3}\left(3S_z^2 - S(S+1)\right) + \frac{E}{2}\left(S_+^2 + S_-^2\right). \qquad \text{eq. S1}$$

This spin Hamiltonian describes six energy levels corresponding to the six possible electronic spin-states, designated -5/2, -3/2, -1/2, 1/2, 3/2, 5/2, with each electronic level being further divided into six sublevels corresponding to the nuclear spin-state. The energies of the six electronic levels are determined by the interaction between the electronic spins and the

laboratory magnet; the Zeeman interaction given by the first term and zero-field interaction given by the last two terms. The energies of the nuclear sublevels are determined by the hyperfine interaction given by the second term. It is this interaction that is responsible for the six sharp fine-structure lines that are often seen in EPR spectra of Mn(II) ions.

It is possible to exploit the Zeeman interaction by using high magnetic-fields to completely spread out the six electronic spin states so that they become essentially evenly spaced at the energy of the applied microwave radiation (Figure 1). This causes a radical simplification of the EPR spectra compared to conventional 9 GHz EPR spectroscopy where the energies of electronic spin levels are determined by the complex interaction of both the Zeeman and zero-field interactions. As shown in Figure 1, the six states deviate from exactly even spacing by multiples of the zero-field interaction. Figure 1 also shows the relationship between these energy levels and the HFEPR spectra observed. For simplicity, we will discuss the case in which $E$ is zero. The EPR spectrum of such a ladder of states is composed of five sets of resonances. One set will be at the magnetic field corresponding to $g\beta B$, which we shall refer to as the center resonance. This center resonance will be flanked by a pair of transitions at $\pm 2D$ relative to the center and another pair $\pm 4D$ from the center. Each of the five sets of resonances will be composed of six hyperfine resonances. In our experiments, this hyperfine structure was observed only in the center transitions and the size of hyperfine couplings was essentially constant. As the zero-field interaction depends on the orientation of the molecule with respect to the applied magnetic-field, the frozen protein solution spectra of the four flanking resonances will be very broad, but distinctly shaped. The zero-field $D$ and $E$ parameter can be obtained from such frozen solution spectra. This is demonstrated in Figure 1 along with the effect of a non-zero $E$.

We could control which of the five transitions we detected by adjusting the temperature. The center transition dominated the spectra obtained at 25 K, while the $-4D$

transition dominated at 4 K. Hence, our measurements were akin to detecting different harmonics by adjusting the temperature. However, unlike real harmonics the information content of each of the transitions is different. The center transition ($m_s$=-1/2→1/2) part of the HFEPR Mn(II) spectra tends to be highly resolved and the center of the spectrum, which defines the Mn(II) *g*-value as well as the hyperfine couplings, can be easily determined. The best way to determine the zero-field parameters, *D* and *E*, depends on the size of the former. For six-coordinate OxdC sites that had relatively small zero-field interactions, the shape of the -4*D* transition was best suited. The *D* and *E* values could be read off from the "turning points" of the spectra (Figure 1). By contrast, for the much larger zero-field interaction of the five-coordinate site for which the $m_s$=-5/2→-3/2 transition was very broad and difficult, if not impossible, to detect with our spectrometer, simulation of center transition based on Eq. S1 worked well. We have previously shown this for manganese superoxide dismutases.[7, 14] As will become apparent in the description of the HFEPR spectroscopy of OxdC centers, both methods, in conjunction with multifrequency spectroscopy, were required to achieve a complete and reliable picture of the pH-dependence.

**3. Equations determining the shape of powder spectra of the $m_s$↔ $m_s$+1 transition.** The resonant-field to first-order in the zero-field parameters is given by

$$B_{res} = \frac{f_{mw} - \left[\frac{3}{2}\left[\frac{D}{3}\left(3\cos^2\theta - 1\right) - E\sin^2\theta\cos^2 2\varphi\right](2m_s + 1)\right]}{g\beta}$$

where $f_{mw}$ is the microwave frequency, θ and ϕ are the polar angles defining the orientation of the magnetic field with respect to the zero-field principal axis system and the rest of symbols are as defined in the text. The hyperfine term has been neglected. For microwave frequencies used in our study, the Zeeman term, $f_{mw}/g\beta$, is much larger than the zero-field contribution. The resonance equation implies that (a) the center of the powder spectrum is defined $f_{mw}/g\beta$ and (b) the width and shape of the powder spectrum to first order is

determined by *D* and *E* and is independent of the observation frequency $f_{mw}$. The second-order terms can be found in references S1 and S2.

## 4. 95 GHz $m_s$=-1/2↔1/2 Spectra of OxdC.

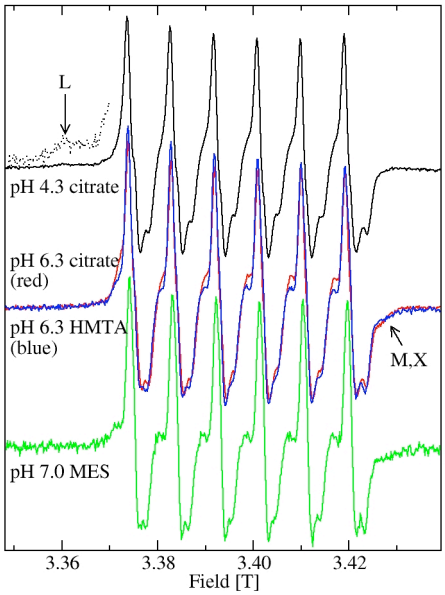


**Figure S2.** The 95 GHz 10 K $m_s$=-1/2↔1/2 spectrum of OxdC as a function of buffer and pH.

## 5. Isotropic hyperfine and g-values of OxdC.

**Table S1.** The Mn(II) isotropic g-values and hyperfine couplings of site-1 and site-2 species. The values were from fits of the spectra of the $m_s$= -1/2↔1/2 transition. The absolute error in the isotropic g value was ±0.0001 (see ref. 30 for details) and hyperfine coupling ±0.005 GHz.

| Species | | Isotropic g | Isotropic Hyperfine Coupling (GHz) |
|---|---|---|---|
| Site-1 | B | 2.00077 | 0.253 |
| citrate | A | 2.00088 | 0.252 |
| Site-2 | H | 2.00080 | 0.250 |
| | M | 2.00080 | 0.251 |
| | L | 2.00086 | 0.251 |
| | $L_2$ | 2.00078 | 0.252 |

**6. Complete citation for reference 29.**

Schwarzenbacher, R., von Delft, F., Jaroszewski, L., Abdubek, P., Ambing, E., Biorac, T., Brinen, L. S., Canaves, J. M., Cambell, J., Chiu, H. J., Dai, X., Deacon, A. M., DiDonato, M., Elsliger, M. A., Eshagi, S., Floyd, R., Godzik, A., Grittini, C., Grzechnik, S. K., Hampton, E., Karlak, C., Klock, H. E., Koesema, E., Kovarik, J. S., Kreusch, A., Kuhn, P., Lesley, S. A., Levin, I., McMullan, D., McPhillips, T. M., Miller, M. D., Morse, A., Moy, K., Ouyang, J., Page, R., Quijano, K., Robb, A., Spraggon, G., Stevens, R. C., van den Bedem, H., Velasquez, J., Vincent, J., Wang, X., West, B., Wolf, G., Xu, Q., Hodgson, K. O., Wooley, J., and Wilson, I. A. (2004) Crystal structure of a putative oxalate decarboxylase (TM1287) from *Thermotoga maritima* at 1.95 A resolution. *Proteins 56*, 392-5.

## Supporting Information References

S1. Taylor, P. C.; Baugher, J. F.; Kriz, H. M., *Chem. Rev.* **1975,** *75*, 203-240.

S2. Bir, G.L., *Sov. Phys. Solid State* **1964**, *5*, 1628-1635.

S3. Swift, L. P.; Cutts, S. M.; Rephaeli, A.; Nudelman, A.; Phillips, D. R., *Mol Cancer Ther* **2002,** *2*, 189-198.